J Neurophysiol 110: 1722–1731, 2013.
First published July 10, 2013; doi:10.1152/jn.00319.2013.

Sniffer patch laser uncaging response (SPLURgE): an assay of regional differences in allosteric receptor modulation and neurotransmitter clearance

Catherine A. Christian and John R. Huguenard
Department of Neurology and Neurological Sciences, Stanford University School of Medicine, Stanford, California

Submitted 6 May 2013; accepted in final form 3 July 2013

Christian CA, Huguenard JR. Sniffer patch laser uncaging response (SPLURgE): an assay of regional differences in allosteric receptor modulation and neurotransmitter clearance. *J Neurophysiol* 110: 1722–1731, 2013. First published July 10, 2013; doi:10.1152/jn.00319.2013.—Allosteric modulators exert actions on neurotransmitter receptors by positively or negatively altering the effective response of these receptors to their respective neurotransmitter. γ-Aminobutyric acid (GABA) type A ionotropic receptors ($GABA_A$Rs) are major targets for allosteric modulators such as benzodiazepines, neurosteroids, and barbiturates. Analysis of substances that produce similar effects has been hampered by the lack of techniques to assess the localization and function of such agents in brain slices. Here we describe measurement of the sniffer patch laser uncaging response (SPLURgE), which combines the sniffer patch recording configuration with laser photolysis of caged GABA. This methodology enables the detection of allosteric $GABA_A$R modulators endogenously present in discrete areas of the brain slice and allows for the application of exogenous GABA with spatiotemporal control without altering the release and localization of endogenous modulators within the slice. Here we demonstrate the development and use of this technique for the measurement of allosteric modulation in different areas of the thalamus. Application of this technique will be useful in determining whether a lack of modulatory effect on a particular category of neurons or receptors is due to insensitivity to allosteric modulation or a lack of local release of endogenous ligand. We also demonstrate that this technique can be used to investigate GABA diffusion and uptake. This method thus provides a biosensor assay for rapid detection of endogenous $GABA_A$R modulators and has the potential to aid studies of allosteric modulators that exert effects on other classes of neurotransmitter receptors, such as glutamate, acetylcholine, or glycine receptors.

GABA; neuromodulation; brain slice; electrophysiology; outside-out patch

ALLOSTERIC MODULATORS of neurotransmitter receptors act by altering the effective response of these receptors to their cognate neurotransmitter in either a positive or a negative direction (Schwartz and Holst 2007). Major classes of such modulators for the ionotropic receptors for γ-aminobutyric acid (GABA), the major inhibitory neurotransmitter in the brain, include benzodiazepines, neurosteroids, barbiturates, and redox agents (Belelli et al. 2006; Calero et al. 2011; Pan et al. 1995; Rudolph and Möhler 2004), which each act at different binding sites on the $GABA_A$ receptor ($GABA_A$R). Assorted $GABA_A$R subunit combinations confer diverse sensitivity to specific modulators (Hadingham et al. 1996; Macdonald and Olsen 1994; Mody and Pearce 2004; Möhler et al. 2001; Pritchett et al. 1989a, 1989b; Wafford et al. 1996). Furthermore, differential expression of endogenous modulators across brain areas and under various physiological states suggests the potential for discrete but functionally powerful effects on overall circuitry.

The GABAergic neurons of the thalamic reticular nucleus (nRT) are a primary source of inhibition in the thalamocortical circuit and provide dense inhibitory projections to the thalamocortical relay cells in the ventrobasal nucleus (VB) (Crabtree et al. 1998; Houser et al. 1980; Jones 1975; Steriade 2005). In addition, nRT neurons inhibit each other (intra-nRT inhibition) via sparse axon collaterals and dendrodendritic connections (Cox et al. 1996; Deschenes et al. 1985; Pinault et al. 1997; Shu and McCormick 2002). The $GABA_A$R α_1-subunit is highly expressed in VB, whereas mature nRT neurons almost exclusively express the α_3-subunit (Fritschy and Mohler 1995; Huntsman et al. 1996; Wisden et al. 1992). In previous work, we observed that the benzodiazepine binding site antagonist flumazenil (FLZ) reduced the duration of spontaneous inhibitory postsynaptic currents (IPSCs) recorded in nRT but not in VB (Christian et al. 2013), suggesting the nucleus-specific localization of endogenous benzodiazepine binding site ligands (endozepines). Our investigations into this question necessitated a technique to assess differences in localization of allosteric modulators in different areas of the thalamus.

To this end, we developed a biosensor for endogenous allosteric modulators of $GABA_A$Rs in brain slices by combining the "sniffer patch" technique (Allen 1997), which has traditionally been used to detect synaptic neurotransmitter release, with GABA uncaging via ultraviolet (UV) laser stimulation, which we have named the sniffer patch laser uncaging response (SPLURgE). Some of the primary data from nRT patches were included in a recent report (Christian et al. 2013); here we present and discuss the development and use of this methodology in further detail. First, we illustrate the inability of sniffer patches pulled from VB neurons to detect electrically evoked release of GABA in nRT, thus requiring an alternative source of GABA that can be applied to these patches in a way that is rapid and spatiotemporally precise. Second, we show that a higher concentration of caged GABA is required to elicit uncaging responses in outside-out patches pulled from nRT cells compared with patches pulled from VB cells, consistent with the concentration dependence observed with rapid GABA application in nRT patches (Schofield and Huguenard 2007). Third, we describe the use of this technique in investigating allosteric modulator expression in the thalamus. Finally, we demonstrate that this technique may also be used to investigate the dynamics of GABA transporter function. This methodology will be useful for detection of allosteric $GABA_A$R modu-

Address for reprint requests and other correspondence: J. R. Huguenard, Dept. of Neurology and Neurological Sciences, Stanford Univ. School of Medicine, 1291 Welch Rd., Alway Bldg. Rm. M016, Stanford, CA 94305 (e-mail: john.huguenard@stanford.edu).

lators and region-specific differences in GABA diffusion or uptake, and should be fruitful for assessment of modulators for other classes of neurotransmitter receptors.

METHODS

Animals. All procedures were approved by the Administrative Panel on Laboratory Animal Care at Stanford University. C57BL/6 mice (Charles River Laboratories, Hollister, CA) of either sex at postnatal days (P)15–35 were used for all experiments. Mice were bred and housed on a 12:12-h light-dark photoperiod with food and water available ad libitum.

Brain slice preparation. Brain slices were prepared according to published procedures (Huguenard and Prince 1994) after deep pentobarbital sodium (55 mg/kg ip) anesthesia. Briefly, the brain was rapidly removed and placed in an oxygenated ice-cold sucrose solution containing (in mM) 234 sucrose, 11 glucose, 26 $NaHCO_3$, 2.5 KCl, 1.25 NaH_2PO_4, 10 $MgSO_4$, and 0.5 $CaCl_2$ (310 mosM). Horizontal brain slices (250 μm) through the somatosensory thalamus were made with a Leica VT1200 microtome (Leica Microsystems, Bannockburn, IL) and incubated in continuously oxygenated artificial cerebrospinal fluid (ACSF) containing (in mM) 10 glucose, 26 $NaHCO_3$, 2.5 KCl, 1.25 $NaHPO_4$, 1 $MgSO_4$, 2 $CaCl_2$, and 120 NaCl (298 mosM). Slices were kept at ~30–32°C for 1 h and then transferred to room temperature (~21–23°C) for at least 15 min before recording.

Patch-clamp electrophysiology and laser uncaging. Slices were individually transferred to a recording chamber on the stage of a Zeiss Axioskop fixed-stage upright microscope (Carl Zeiss, Thornwood, NY) continuously superfused at 2 ml/min with oxygenated ACSF at room temperature. Whole cell patch-clamp recordings were made with a MultiClamp 700A amplifier with Clampex 9.2 software, and signals were digitized with a Digidata 1322A (Molecular Devices, Sunnyvale, CA). Borosilicate glass recording pipettes were prepared with a model P-97 Flaming/Brown micropipette puller (Sutter Instrument, Novato, CA) to 2.5- to 4-MΩ tip resistance when filled with an isotonic chloride intracellular pipette solution, which contained (in mM) 135 CsCl, 10 HEPES, 10 EGTA, 2 $MgCl_2$, and 5 QX-314, pH adjusted to 7.3 with CsOH (290 mosM). Where indicated, 5 mM MgATP was added to the internal solution immediately prior to use. All recordings were made in the presence of D-(−)-2-amino-5-phosphonovaleric acid (APV, 100 μM; Ascent Scientific, Princeton, NJ) plus 6,7-dinitroquinoxaline-2,3-dione (DNQX, 20 μM; Ascent Scientific) to isolate $GABA_A$R-mediated currents. For uncaging experiments, α-carboxy-2-nitrobenzyl ester (CNB)-caged GABA (100 μM–1 mM; Invitrogen, Carlsbad, CA) was added to a 15-to 20-ml recirculating bath ACSF solution. In some cases 1 μM FLZ (Sigma-Aldrich, St. Louis, MO) and/or the GABA transporter (GAT) antagonists 1,2,5,6-tetrahydro-1-[2-[[(diphenylmethylene)amino]oxy]ethyl]-3-pyridinecarboxylic acid hydrochloride (NNC 711, 4 μM; Tocris Bioscience, Minneapolis, MN) and 1-[2-[*tris*(4-methoxyphenyl)methoxy] ethyl]-(*S*)-3-piperidinecarboxylic acid [(*S*)-SNAP 5114, 10 μM; Tocris Bioscience] were included in the ACSF bath solution. For the experiments in Fig. 1, electrical stimuli were delivered via a bipolar tungsten electrode placed in nRT.

Outside-out membrane patches were pulled from neurons with established procedures (Hamill et al. 1981; Sakmann and Neher 2009). Briefly, a whole cell recording was established with the membrane holding potential (V_m) set at −60 mV. V_m was then set at −30 mV, followed by slow withdrawal of the patch electrode until a cell-free patch of membrane was isolated on the pipette tip, which ensured stability of the resultant outside-out patch. The pipette tip was fully removed (>50 μm) from the slice in order to completely excise the patch from the original cell. The peak patch input resistance was ~1–2 GΩ. Patches with input resistance < 100 MΩ were less stable and either ruptured upon placement into the slice or exhibited very low amplitude and unstable uncaging responses. Sniffer patches were placed in the slice to a depth at which nearby cell bodies could be clearly visualized (~25–50 μm). Where indicated, some responses were recorded from patches positioned above the slice. For the experiments in Figs. 5 and 6, precise patch placement depth was determined by positioning the tip of the pipette at the surface of the slice and setting the *z*-axis value on the micromanipulator (MP-285; Sutter Instrument) to 0 for each patch. One-millisecond-duration UV light pulses (20 μW) were delivered with a 355-nm-wavelength laser beam (DPSS Lasers, Santa Clara, CA) directed into the epifluorescence port of the microscope and through the back aperture of a ×60 water immersion objective. The pipette tip was placed in the center of the focused laser spot to ensure maximal photolysis of ambient caged GABA. Placement of the pipette 25 μm below the plane of the focus was sufficient to completely abolish the uncaged GABAergic current. Final localization of the patch electrode tip in VB or nRT was confirmed by capturing a video frame from the microscope with a ×2.5 or ×10 objective to visualize pipette placement. Recordings were made in voltage-clamp mode with 20 mV/pA gain, sampled every 40 μs, and low-pass Bessel filtered at 2 kHz.

Data analysis. Recordings were analyzed with Clampfit 9.2 software (Molecular Devices), and data were exported to Excel (Microsoft, Redmond, WA) and Origin 7 (Microcal Software, Northampton, MA) for statistical analysis. In Clampfit, traces were low-pass Boxcar filtered post hoc at 99 smoothing points. The peak amplitude, half-width, 10–90% rise time, and 90–10% decay time of the responses were calculated with the Statistics protocol in Clampfit. Two-tailed paired *t*-tests were used for comparisons of values for the third vs. the first responses in individual patches and for comparisons of responses obtained up to 50 μm into the slice with those obtained 50 μm above the slice. The third response was chosen for comparison because at least three responses were readily obtained from each patch. Comparisons between VB and nRT patches and between responses obtained in control vs. GAT blockade conditions were made with two-tailed independent *t*-tests. Comparison of amplitude ratios obtained at 10-s, 30-s, and 60-s interstimulus intervals (ISIs) (see Fig. 2) was performed with one-way ANOVA. A Fisher's exact test was used for the statistical comparison in Fig. 1*D*. Statistical significance was set at $P < 0.05$. Data are presented as means ± SE.

RESULTS

Patches pulled from VB neurons can detect electrically evoked GABA release in VB but not nRT. The ability of outside-out membrane patches pulled from VB neurons to detect GABA released synaptically (Banks and Pearce 2000; Isaacson et al. 1993) was tested by placing these patches back in the slice in either VB or nRT to act as "sniffer" patches (Allen 1997) (Fig. 1*A*) and electrically evoking GABA release via a stimulating electrode placed in nRT. VB patches were chosen because previous work using rapid GABA application indicated that $GABA_A$Rs in patches from VB neurons exhibit higher channel density and affinity for GABA than those from nRT neurons (Schofield and Huguenard 2007), and thus would be more likely to detect synaptic GABA release. Indeed, small-amplitude (<10 pA) synaptically evoked responses were detectable in VB (responses observed in 5 of 8 patches tested; example in Fig. 1*B*), but when patches were placed in nRT responses were undetectable (responses were not observed in any of 8 patches; Fig. 1*C*, $P < 0.05$, Fisher's exact test). The increased probability of detecting synaptic GABA release in VB compared to nRT is likely due to the greater GABAergic innervation of VB compared with the relatively sparse innervation within nRT (Cox et al. 1996; Pinault et al. 1997).

Because the synaptic release of GABA was not detectable by these means with patches placed in nRT, we decided to take the

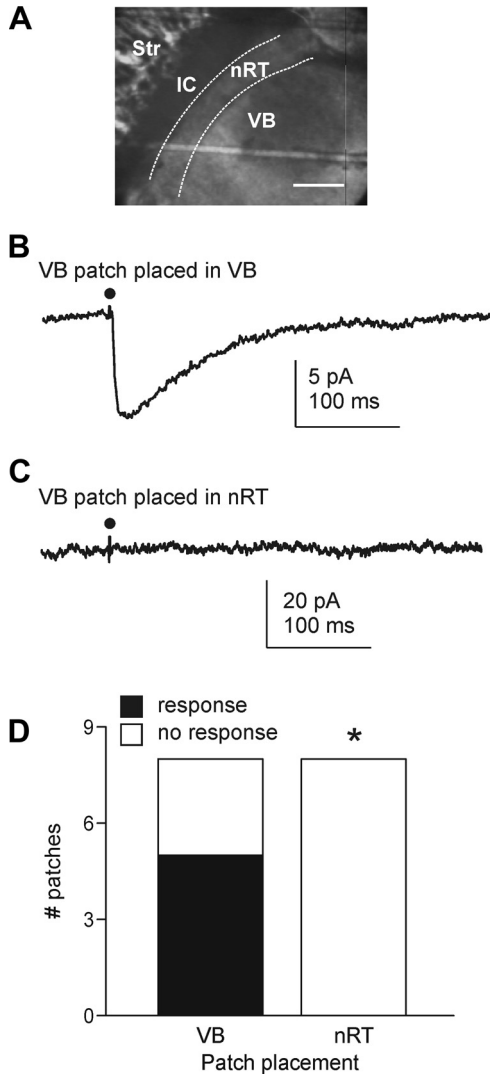

Fig. 1. GABA release in thalamus evoked by electrical stimulation in thalamic reticular nucleus (nRT) can be detected by ventrobasal nucleus (VB) membrane patches placed in VB but not in nRT. *A*: example microscope image of a horizontal thalamic slice showing positions of nRT (outlined by white dashed lines) and VB. Calibration bar, 250 μm. IC, internal capsule; Str, striatum. *B*: representative averaged evoked GABAergic response (35-V stimulation in nRT) of an outside-out sniffer patch pulled from a VB neuron and placed back in VB. Black dot indicates time of electrical stimulation applied to nRT. The illustrated response is typical of that observed in 5 of 8 patches tested. *C*: representative averaged response of a patch pulled from a VB neuron and then placed in nRT (40-V stimulation). Example chosen from 8 patches tested. Electrical stimulation artifacts have been truncated for clarity. *D*: stacked bar chart illustrating rate of response of sniffer patches pulled from VB neurons to electrical stimulation when placed in VB or nRT. *$P < 0.05$, Fisher's exact test.

approach of providing an external source of GABA. Although rapid GABA application or puffs could potentially be used in this fashion, the mechanical shock associated with these methods could compromise the stability and reproducibility of responses from patch to patch. By contrast, laser uncaging of GABA results in rapid transients in GABA concentration in the region of the focused beam without mechanical artifacts. Furthermore, because the caged GABA is applied via the bath solution, penetration into the extracellular space throughout the depth of the slice and across different regions facilitates comparison of responses across different brain areas.

Patches pulled from nRT and VB cells show nucleus-specific differences in affinity to laser-uncaged GABA. The affinity of VB and nRT patches to laser-uncaged GABA was tested by recording the responses to 1-ms laser stimuli in the presence of different ambient concentrations of caged GABA. At 100 μM caged GABA, VB patches exhibited high-amplitude (-96.26 ± 8.23 pA) responses that had a rapid onset (10–90% rise time 17.34 ± 3.25 ms) and slower decay profile that could be fit to a double-exponential function, typical of postsynaptic currents ($n = 7$ patches; example in Fig. 2*A*). nRT patches, however, showed smaller-amplitude (17.56 ± 7.91 pA), slow-onset (121.51 ± 60.99 ms) responses at this concentration ($n = 3$ patches; example in Fig. 3*A*). When the caged GABA concentration was increased to 1 mM, however, nRT patches showed responses that were much higher amplitude (~2-fold, 40.84 ± 10.96 pA) and faster onset (24.95 ± 2.22 ms) and more closely resembled the kinetics and amplitude of IPSCs ($n = 8$ patches; example in Fig. 3*B*). These findings are consistent with nRT patches expressing $GABA_A$ receptors with lower affinity than patches from VB cells, as previously demonstrated with rapid GABA application to outside-out patches (Schofield and Huguenard 2007), though the duration of uncaging responses in both VB and nRT patches was approximately four to five times longer than those obtained with rapid application. The duration of the response of nRT patches was two- to fivefold longer than that of VB patches ($P < 0.001$) (Fig. 2, *A* and *B*, Fig. 3, *B* and *C*), consistent with the longer time course of nRT spontaneous IPSCs (Browne et al. 2001; Christian et al. 2013; Huntsman et al. 1999; Schofield et al. 2009; Zhang et al. 1997) and responses to transient GABA application (Schofield and Huguenard 2007).

Amplitude of GABA uncaging response in patches progressively decreases with successive stimulations, but decay rate is stable. We observed a progressive decrease in the amplitude of the response of patches pulled from either VB or nRT neurons to GABA uncaging over successive trials when laser stimuli were delivered at 10-s intervals (Fig. 2, *B* and *C*, Fig. 3, *C* and *D*). Initial response amplitude was variable from patch to patch, potentially resulting from differences in patch input resistance, patch size, and/or the number of receptors located within each patch. The decay properties of responses in these same patches, however, were relatively stable (Fig. 2, *B* and *C*, Fig. 3, *C* and *D*, $P > 0.1$), indicating that several responses can be obtained from the same patch and used in kinetics analyses.

It is possible that the decrease in amplitude reflects desensitization of the receptors, which does not recover within the 10-s window between laser stimuli. When laser pulses were given at either a 30-s ($n = 4$ patches) or a 60-s ($n = 3$ patches) ISI, however, the progressive reduction persisted (Fig. 2, *D–F*). The degree of this reduction was not significantly different between patches stimulated at 10-s, 30-s, or 60-s ISIs ($F = 0.36$, $P > 0.7$). Therefore, it appears that the reduced amplitude over successive trials every 10 s is not due to an insufficient ISI duration.

Rundown of uncaging response amplitude in VB neurons is ameliorated by replenishment of caged GABA. To determine whether the rundown of uncaging response amplitudes observed in pulled patches is an artifact of the patch recording configuration, we performed whole cell recordings of VB neurons under the same conditions of uncaging stimuli as performed on patches. Although the degree of rundown was

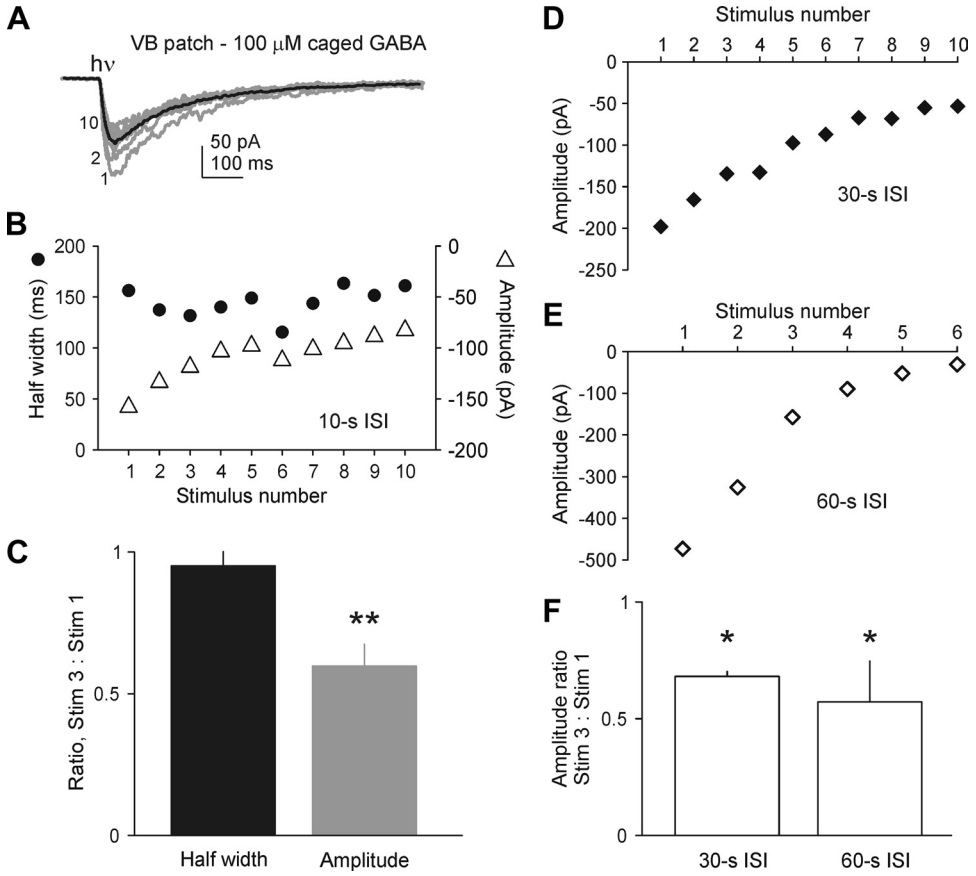

Fig. 2. Responses of VB patches to laser photolysis of caged GABA when patches are held above the slice. *A*: representative example of uncaging responses in a VB patch in the presence of 100 μM caged GABA. Gray traces represent individual sweeps elicited every 10 s, and black trace is the composite average. Numbers on *left* of gray traces indicate the order of responses elicited. hν, 1-ms UV laser stimulus. *B*: individual uncaged inhibitory postsynaptic current (IPSC) half-width and amplitude values for each sweep in the example in *A*. ISI, interstimulus interval. *C*: mean + SE ratio of the uncaged IPSC half-width or amplitude in response to 3rd laser stimulus to the respective value of the response to 1st stimulus, averaged across 6 patches. *D*: individual uncaged IPSC amplitude values for an example VB patch with uncaging responses elicited every 30 s. *E*: individual uncaged IPSC amplitude values for an example VB patch with uncaging responses elicited every 60 s. *F*: mean + SE ratio of the uncaged IPSC amplitude in response to 3rd laser stimulus to the respective value of 1st stimulus, averaged across 4 patches (30-s ISI) or 3 patches (60-s ISI). $*P < 0.05$, $**P < 0.01$, paired *t*-test within patches vs. response to 1st stimulus.

not as steep as that seen in patches, there was a significant decrease in response amplitude by the fifth stimulus when given at a 10-s ISI ($n = 8$ cells) (Fig. 4*A*). This was not improved by inclusion of 5 mM MgATP (Kaneda et al. 1995) in the pipette internal solution ($n = 6$ cells). We did observe a positive correlation, however, between the degree of rundown and the order in which each cell was recorded relative to the last application of new caged GABA ($P < 0.05$) (Fig. 4*B*). This suggests that the amplitude rundown is not a result of recording in pulled patches, but as "liberated" GABA and/or cage compound accumulates in the bath solution, these can interfere with the amplitude of the uncaging responses. These effects can therefore be reduced by minimizing recirculation of the uncaging solution.

GABA transport differentially affects early and late decay kinetics of SPLURgEs. The results presented in Figs. 2 and 3 describe the responses to laser uncaging obtained when patches are held outside of the slice, and thus away from potential influences of modulation or altered diffusion or uptake. Placement of patches within the slice, which confers the designation of "sniffer patch" (Allen 1997), allows for investigation of these factors by measurement of the SPLURgE. Properties of SPLURgEs in VB patches were tested by pulling patches from VB neurons and placing them back in the slice either in VB or in nRT, typically ~25–50 μm into the slice, before uncaging GABA onto the patch. Placement of patches in the slice was not detrimental to patch quality or SPLURgE stability (Fig. 5, *A* and *B*; $P > 0.1$ for the ratio of the SPLURgE half-width in response to the 3rd laser stimulus to the respective value of the response to the 1st stimulus, $n = 5$).

We hypothesized that SPLURgE kinetics would be affected by differential GABA diffusion and/or uptake in and out of the slice. Diffusion will be slowed within the slice compared with in free solution because of cellular elements that hinder movement of solutes in the microenvironment of the brain (Syková and Nicholson 2008). In addition, GATs, which are present within, but not outside, the slice, may play a major role in determining the kinetic profile of the SPLURgE, acting to reduce duration by speeding the elimination of uncaged GABA. To examine these possibilities, we tested the SPLURgE response in and out of VB, where FLZ-sensitive allosteric modulation does not appear to occur (Christian et al. 2013).

In the following experiments, uncaging responses were obtained as the patch was moved sequentially along the *z*-axis into the tissue to obtain at least one response at each *z*-axis

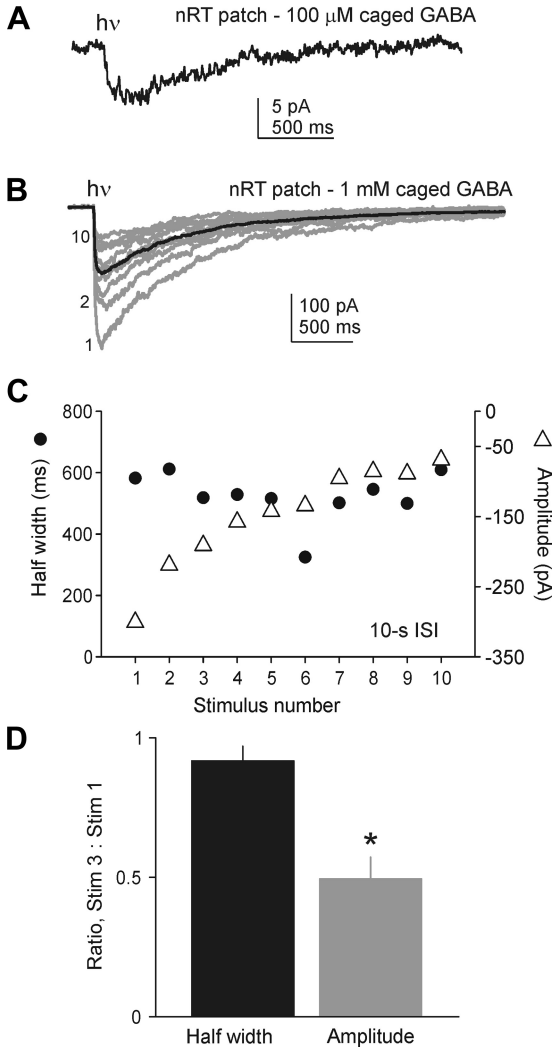

Fig. 3. Responses of nRT patches to laser photolysis of caged GABA when patches are held above the slice. *A*: representative example of averaged uncaging response in an nRT patch in the presence of 100 μM caged GABA. Example chosen from 3 patches tested. hν, 1-ms UV laser stimulus. *B*: representative example (from 8 patches) of uncaging responses obtained every 10 s in an nRT patch in the presence of 1 mM caged GABA. Gray traces represent individual sweeps, and black trace is the composite average. Numbers on *left* of gray traces indicate the order of responses elicited. *C*: individual uncaged IPSC half-width and amplitude values for each sweep in the example in *B*. *D*: ratio of uncaged IPSC half-width or amplitude in response to 3rd laser stimulus to the respective value of the response to 1st stimulus, averaged across 5 patches. *$P < 0.05$, paired *t*-test within patches vs. response to 1st stimulus.

position. As patch health permitted, this process was reversed to obtain additional responses. Where possible, multiple responses at each *z*-axis position were averaged to obtain the mean value for a given parameter at a particular *z*-axis position. These values were then normalized to the mean value obtained at -50 μm above the slice. In control conditions, the time course of SPLURgEs was accelerated when patches were placed within the slice compared with when patches were recorded above the slice (Fig. 5*C*). When patches were placed into the slice, SPLURgE duration decreased such that the decay time, but not the half-width, was significantly reduced ($P < 0.05$) compared with values obtained when the same patches were recorded above the slice (Fig. 5, *E* and *F*). Consistent with the hypothesis that GAT activity affects SPLURgE duration, this relationship was reversed when the GAT-1 blocker NNC 711 and the GAT-3 blocker (*S*)-SNAP 5114 were included in the bath solution. Under these conditions, SPLURgE response duration was instead increased when patches were placed within the slice (Fig. 5*D*). Specifically, SPLURgE half-width displayed a greater degree of enhancement, whereas the decay time was not significantly different from values obtained above the slice (Fig. 5, *E* and *F*). When SPLURgEs were obtained in patches held above the slice, GAT blockade produced no change in either half-width or 90–10% decay time ($P > 0.5$) compared with control conditions. By contrast, when patches were placed within the slice, both the half-width and decay time were significantly increased ($P < 0.01$) by GAT blockade treatment compared with control (Fig. 5, *E* and *F*). These results suggest that diffusion and GAT-mediated GABA uptake differentially affect the early and late decay kinetics of uncaging responses.

SPLURgE duration in VB patches is potentiated when patches are placed in nRT. When patches were placed in nRT, the SPLURgE was significantly potentiated compared with that

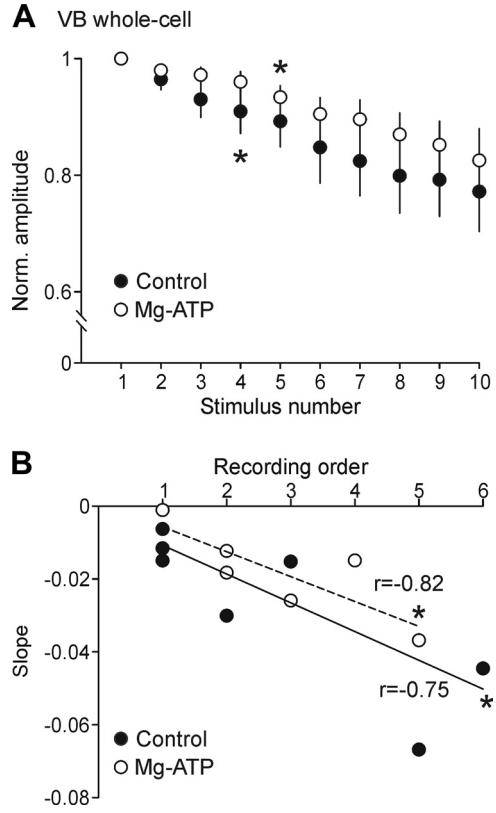

Fig. 4. Uncaged GABA response rundown occurs similarly in whole cell vs. isolated patch mode, and is not rescued by inclusion of Mg-ATP in the pipette, but the degree of rundown increases progressively with each successive recording after introduction of new caged GABA solution. *A*: mean ± SE uncaged IPSC amplitude over successive trials normalized to the amplitude of 1st uncaging response in each cell obtained at a 10-s ISI when cells were filled with either control CsCl internal solution or CsCl with additional 5 mM MgATP. *B*: individual values for each cell of the slope of the line of best fit through the normalized amplitude values over 10 successive trials. Linear regression lines of best fit show positive correlations between recording order after fresh caged GABA replacement and the slope of rundown response. Solid line indicates the line of best fit for all control values, and dashed line indicates the line of best fit for cells recorded with MgATP in the pipette solution. *$P < 0.05$, paired *t*-test within cells vs. response to 1st stimulus (*A*); Pearson correlation (*B*).

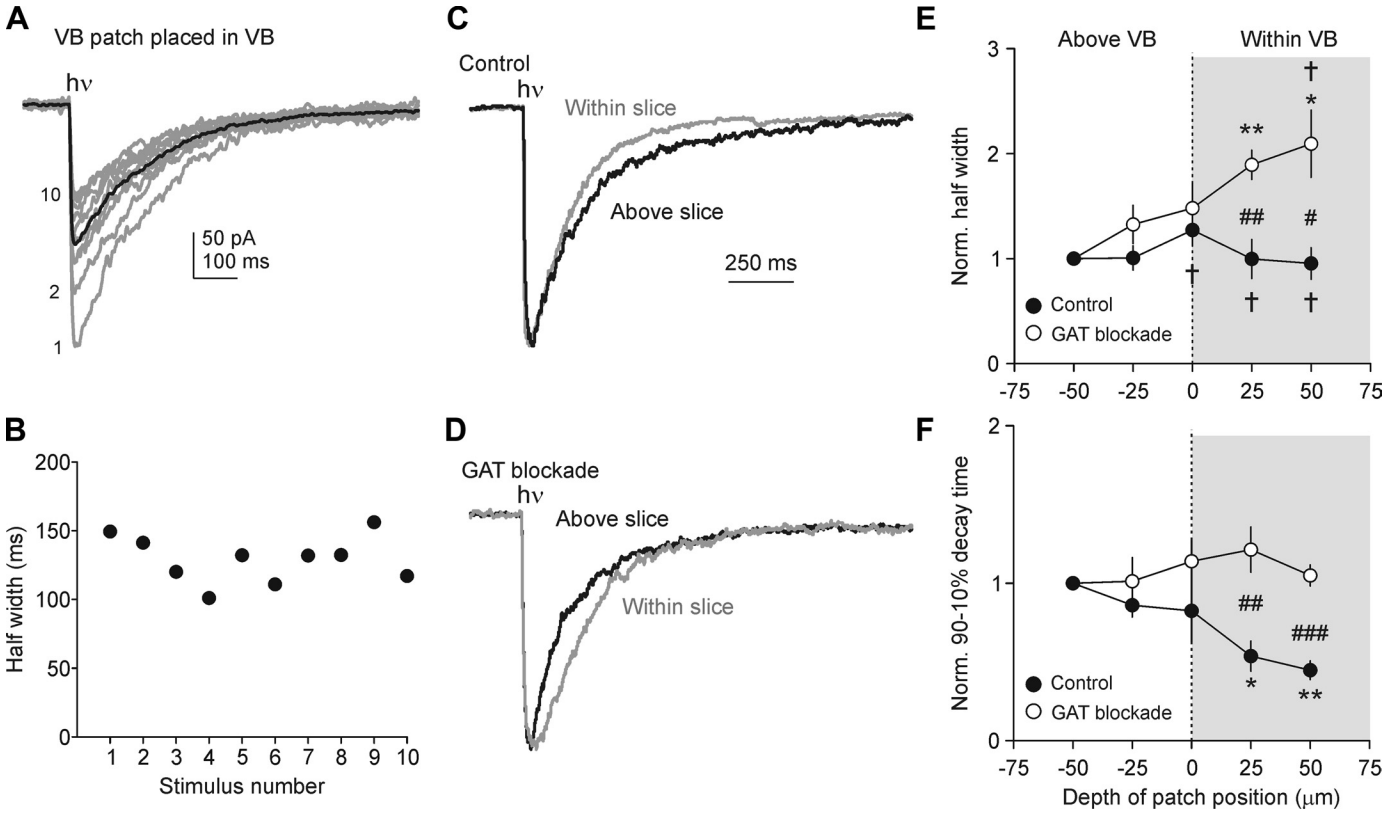

Fig. 5. GABA diffusion and uptake differentially regulate the early and late decay kinetics of sniffer patch laser uncaging responses (SPLURgEs), respectively. *A*: representative example of SPLURgEs in a VB patch in the presence of 100 μM caged GABA when the patch is placed back in the slice in VB. Gray traces represent individual sweeps elicited every 10 s, and black trace is the composite average. Numbers on *left* of gray traces indicate the order of responses elicited. hν, 1-ms UV laser stimulus. Note here that all responses were obtained with the patch positioned within the slice. *B*: individual SPLURgE half-width values for each sweep in the example in *A*. *C* and *D*: averaged SPLURgE traces from VB patches placed above the slice (black traces) and in the slice in VB (gray traces) under control conditions (*C*) or under conditions of pharmacological GABA transporter (GAT) blockade (*D*). Traces were obtained in the presence of 100 μM caged GABA and normalized to peak amplitude. *E* and *F*: mean ± SE SPLURgE half-width (*E*) and 90–10% decay time (*F*) as a function of *z*-axis placement of pipette relative to the surface of the brain slice for VB patches placed back within VB in control conditions (4 patches) or in the presence of GAT blockers (4 patches). Responses are normalized to the values obtained −50 μm above the slice for each patch. $^{*}P < 0.05$, $^{**}P < 0.01$, paired *t*-test within patches vs. response at −50 μm above slice; $^{\#}P < 0.05$, $^{\#\#}P < 0.01$, $^{\#\#\#}P < 0.001$, *t*-test vs. control at respective position depth; †$P < 0.05$, paired *t*-test within patches vs. normalized 90–10% decay time values at respective position depth.

obtained in patches placed in VB (Fig. 6*A*), suggesting differences in GABA diffusion, uptake, or allosteric modulators between the two nuclei. We have previously demonstrated that this potentiation represents a combination of *1*) allosteric modulation that is sensitive to the benzodiazepine binding site antagonist FLZ, suggesting that this potentiation is due at least in part to the actions of an endogenous positive allosteric benzodiazepine site agonist in nRT, and *2*) slower GABA uptake in nRT than in VB (Christian et al. 2013). Our previous work used mice on the 129/SvEvTac background; here we extend this finding to the C57BL/6 strain.

To further calibrate the SPLURgE above vs. within nRT, patches were pulled from VB neurons and recorded when positioned from 25 μm above to 50 μm deep into the slice. In patches recorded under control conditions, SPLURgE duration progressively increased as the patch was placed more deeply in nRT (n = 4 patches; Fig. 6, *B* and *C*). In the presence of FLZ, however, the increase in duration was blocked and SPLURgE 90–10% decay time was significantly decreased with deeper placement within the slice (n = 4 patches; Fig. 6, *B* and *C*). These results support and extend our previous observations that the nRT-dependent potentiation of the uncaging response largely reflects actions of endogenous allosteric modulators acting on $GABA_AR$ benzodiazepine binding sites (Christian et al. 2013). Furthermore, it should be noted that the differential effects of patch placement within the slice on half-width vs. 90–10% decay time in the presence of FLZ (i.e., when endozepine modulation is blocked) are similar to what was observed when VB patches were placed in VB (Fig. 5), where endozepines do not appear to be released (Christian et al. 2013). Thus it is likely that in nRT, as in VB, the SPLURgE profile that is independent of endozepine modulation reflects a combination of GAT-mediated uptake, preferentially affecting the late decay kinetics, and diffusion, which contributes to the early decay parameter.

DISCUSSION

Here we describe a new methodology for detecting region-specific differences in GABA receptor function in brain slices, which we have used to detect localized expression of endozepines, endogenous benzodiazepine site ligands. By combining the sniffer patch recording configuration with GABA uncaging, stereotyped transient GABA increases can be reproduced in different nuclei. In addition to allosteric modulation, this method could potentially be used to investigate regional differences in extracellular space volume fraction, tortuosity,

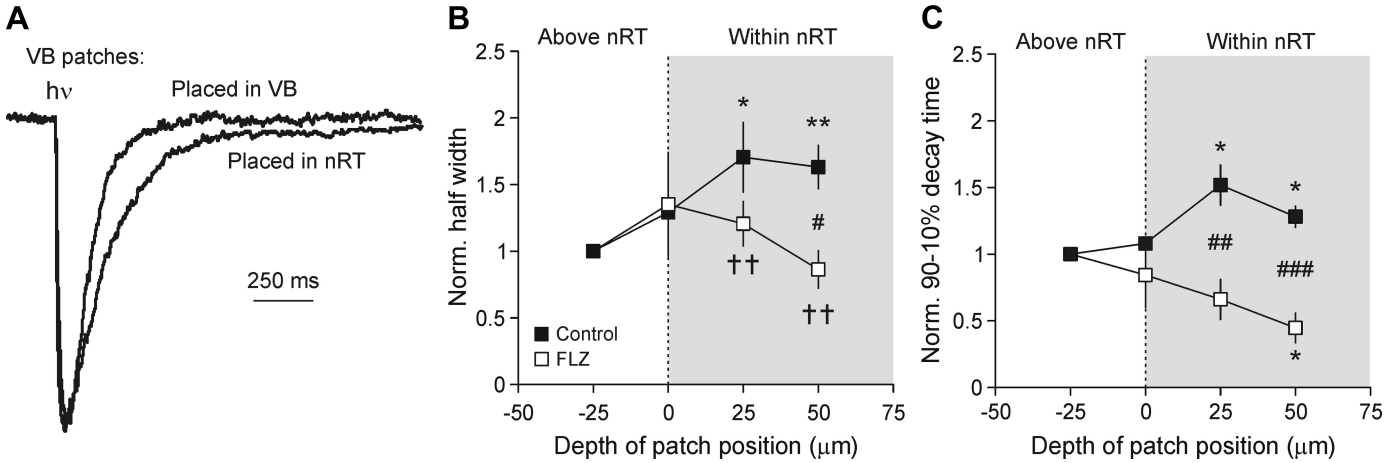

Fig. 6. SPLURgE potentiation in patches pulled from VB neurons and placed in nRT is flumazenil (FLZ) sensitive and dependent on depth of patch placement. *A*: averaged SPLURgE traces from representative individual VB patches placed in VB or nRT in the presence of 100 μM caged GABA, normalized to peak amplitude. hν, 1-ms UV laser stimulus. *B* and *C*: mean ± SE SPLURgE half-width (*B*) and 90–10% decay time (*C*) as a function of *z*-axis placement of pipette relative to the surface of the brain slice for example VB patches placed in nRT in control conditions (4 patches) or in the presence of 1 μM FLZ (4 patches). Responses are normalized to the values obtained more than −25 μm above the slice for each patch. $^{*}P < 0.05$, $^{**}P < 0.01$, paired *t*-test within patches vs. response at more than −25 μm above slice; $^{\#}P < 0.05$, $^{\#\#}P < 0.01$, $^{\#\#\#}P < 0.001$, *t*-test vs. control at respective position depth; $\dagger\dagger P < 0.01$ paired *t*-test within patches vs. normalized 90–10% decay time values at respective position depth.

diffusion, and uptake (Syková and Nicholson 2008). The advantage of providing an exogenous source of GABA is illustrated by the ability of patches pulled from VB neurons to robustly detect responses even under conditions in which synaptic release of GABA was undetectable.

The durations of uncaging responses for patches pulled from neurons in both nuclei were longer than those for spontaneous or evoked IPSCs, consistent with previous studies on patches pulled from thalamic, hippocampal, and cortical neurons (Banks and Pearce 2000; Galarreta and Hestrin 1997; Jones and Westbrook 1997; Perrais and Ropert 1999; Schofield and Huguenard 2007). The longer time course for responses in nRT patches is in accordance with the longer time course of IPSCs (Browne et al. 2001; Huntsman et al. 1999; Zhang et al. 1997) in nRT compared with VB, and likely reflects nucleus-specific differences in receptor subunit composition (Fritschy and Mohler 1995; Huntsman et al. 1996; Wisden et al. 1992) and resultant differences in GABA affinity and unbinding (Schofield and Huguenard 2007). The mechanism underlying increased duration of currents in patches vs. neurons remains unclear, although alterations in interactions of cytoskeletal elements or intracellular modulators with $GABA_A$Rs (Petrini et al. 2003; Wang et al. 1999) may play a role.

Both the rise times and duration were longer for uncaging responses than the values previously observed with rapid (2 ms) 1 mM GABA application (Schofield and Huguenard 2007). Methodological differences between the two studies, such as alterations in patch holding potential and ionic composition of pipette solutions, may account for this. Alternatively, it is more likely that variations in the spatiotemporal profile of GABA application between the two methods underlie these differences. The rapid GABA application method uses a piezoelectric transducer to expose the patch to control or ligand-containing solutions, and the duration of ligand exposure is determined by the rate of switching between the two solutions. As demonstrated here in the SPLURgE method, by contrast, the time course of ligand exposure evoked by UV uncaging can be influenced by factors such as neurotransmitter uptake and diffusion and is almost certainly longer than that achieved with rapid application, as evidenced by the longer responses obtained with uncaging. For experiments requiring higher spatiotemporal uncaging control, the SPLURgE technique could potentially be modified by using a two-photon laser to uncage the ligand onto the patch, although the current lack of information about the precise dynamics of the GABA concentration transient remains a limitation of the SPLURgE technique.

Another general limitation of using pulled patches is that the membrane arises from the soma and the relative content of synaptic vs. extrasynaptic receptors is not known. In thalamic relay neurons, synaptic receptors are composed of $\alpha_1\beta_2\gamma_2$ $GABA_A$ receptor heteromers, whereas extrasynaptic receptors are $\alpha_4\beta_2\delta$ (Jia et al. 2005; Porcello et al. 2003; Sur et al. 1999). Given that the latter are insensitive to benzodiazepine modulation (Rudolph and Möhler 2004), the augmentation of $GABA_A$ responses by nRT-derived endozepines in thalamic patches indicates that the sniffer patches do contain, at least in part, synaptic-type receptors. Nevertheless, the longer transient of GABA availability at the receptors in the SPLURgE technique may provide further applications for examination of extrasynaptic signaling mechanisms, which are more highly regulated by transporters (Beenhakker and Huguenard 2010).

The amplitude of uncaging responses was consistently observed to progressively decrease over subsequent UV stimuli in both VB and nRT patches. In whole cell recordings in VB neurons, which also displayed a significant rundown of uncaging response amplitude, the degree of this effect could be ameliorated by replacement of the used caged GABA solution (which over time will contain more accumulated GABA, cage molecules, and perhaps other by-products) with fresh caged GABA. Therefore, in cases where experimenters require as little rundown as possible, the caged GABA solution could be replenished before each recording, although this may be prohibitively expensive in many cases, especially where high concentrations are required.

The time required to move the pipette to nRT was typically <10 s. Given that decay properties of VB patch responses to GABA uncaging are stable across many trials (Figs. 2 and 5), it is unlikely that this delay accounts for the potentiation of the uncaging current. Furthermore, FLZ largely blocked the potentiation, demonstrating that endozepine actions play a major role in this difference. In addition, once the pipette was positioned over the nRT portion of the slice, the same amount of time was required to place the pipette within the slice as when the patch was placed in VB. It therefore appears that allosteric potentiation of GABAergic currents occurs on a fast timescale depending on the diffusion and binding of a given modulator to the affected $GABA_A$Rs, although the rate of modulation detected by the SPLURgE likely depends on the combination of $GABA_A$R subunits and allosteric modulators in question. It is conceivable, however, that this technique could be used to understand the dynamics of allosteric modulation in cases in which this interaction occurs on a much slower timescale.

In addition to investigations into allosteric receptor modulation, we also demonstrate that this technique may be used to ascertain properties of GABA diffusion and uptake in brain slices. The altered profile of responses obtained at different positions along the *z*-axis within and above the slice suggests that GAT activity speeds up the decay kinetics of SPLURgEs by removing uncaged GABA and, conversely, that decreased GABA diffusion slows some SPLURgE decay properties. In control conditions, the half-width parameter was not significantly affected by placement in the slice but the 90–10% decay time was significantly shortened as the patch was placed more deeply into the slice. In GAT blockade conditions, however, SPLURgE half-width significantly increased with placement in the slice, whereas decay time was not altered by *z*-axis position. This finding suggests that the early decay times of SPLURgEs reflect opposing forces: *1*) factors that would increase response duration such as tissue tortuosity, decreased volume fraction (Syková and Nicholson 2008), and/or a gradient of GABA concentration through the depth of the slice and *2*) GAT-mediated uptake, which acts strongly to decrease response duration. The late decay component, on the other hand, appears primarily determined by the rate of GAT uptake. This is consistent with previous findings that GAT activity plays a critical role in determining the kinetics of $GABA_B$ IPSCs (Beenhakker and Huguenard 2010; Isaacson et al. 1993; Scanziani 2000; Thompson and Gähwiler 1992), which are similarly long-lasting. In addition, slight changes in SPLURgE duration with positioning closer to the surface of the slice (Fig. 5) indicate that this technique could potentially be used to investigate properties of the "unstirred layer" at the surface of the slice (Hall et al. 2012; Lipinski and Bingmann 1987). The powerful effects of GAT activity to decrease SPLURgE duration through removal of extracellular GABA also suggest that the degree of allosteric modulation in nRT (which acts in this case to increase SPLURgE duration) is partially masked by GAT uptake and may in fact be greater than observed by these methods.

Here we have focused on $GABA_A$R modulation, but the SPLURgE methodology, with minor modifications, could theoretically be applied to the study of other neurotransmitter receptors as well. For example, glutamate receptors in patches pulled from dendrites (Davie et al. 2006) or somata (O'Connor et al. 1995) could be exposed to uncaged glutamate to detect endogenous modulators mimicking compounds that act allosterically at AMPA, NMDA, and metabotropic glutamate receptors (Costa et al. 2010; Fucile et al. 2006; Mony et al. 2009; Sheffler et al. 2011; Yang and Svensson 2008). Similarly, acetylcholine, glycine, and serotonin receptors are also targets for allosteric modulation (Collins et al. 2011; Davies 2011; Faghih et al. 2008; Johnstone et al. 2011; Karakas et al. 2011; Léna and Changeux 1993; Yévenes and Zeilhofer 2011) and could potentially be studied with this technique.

In summary, a major advantage of the SPLURgE method, which combines the "sniffer patch" recording configuration with laser photolysis of caged GABA, is relatively rapid assessment of local differences in $GABA_A$R function. Furthermore, the ability to move receptors contained within membrane patches from one brain area to another provides a way to determine whether a lack of modulatory effect on a particular category of neurons or receptors is due to insensitivity to such modulation or a lack of local release of endogenous ligand. This technique should therefore be useful in applications for rapid detection of $GABA_A$R modulators, as well as allosteric modulators that act on other classes of ionotropic receptors.

ACKNOWLEDGMENTS

We thank Anne Herbert, Kathy Peng, and Corinne Badgley for assistance with mouse colony maintenance.

GRANTS

This work was supported by National Institute of Neurological Disorders and Stroke (NINDS) R01 Grants NS-034774 and NS-006477. C. A. Christian was supported by NINDS Institutional Postdoctoral Training Grant T32 NS-007280, an Epilepsy Foundation of America Postdoctoral Research Fellowship, and a Katharine McCormick Advanced Postdoctoral Fellowship from Stanford School of Medicine.

DISCLOSURES

No conflicts of interest, financial or otherwise, are declared by the author(s).

AUTHOR CONTRIBUTIONS

Author contributions: C.A.C. and J.R.H. conception and design of research; C.A.C. performed experiments; C.A.C. analyzed data; C.A.C. and J.R.H. interpreted results of experiments; C.A.C. prepared figures; C.A.C. drafted manuscript; C.A.C. and J.R.H. edited and revised manuscript; C.A.C. and J.R.H. approved final version of manuscript.

REFERENCES

Allen TG. The "sniffer-patch" technique for detection of neurotransmitter release. *Trends Neurosci* 20: 192–197, 1997.

Banks MI, Pearce RA. Kinetic differences between synaptic and extrasynaptic $GABA_A$ receptors in CA1 pyramidal cells. *J Neurosci* 20: 937–948, 2000.

Beenhakker MP, Huguenard JR. Astrocytes as gatekeepers of $GABA_B$ receptor function. *J Neurosci* 30: 15262–15276, 2010.

Belelli D, Herd MB, Mitchell EA, Peden DR, Vardy AW, Gentet L, Lambert JJ. Neuroactive steroids and inhibitory neurotransmission: mechanism of action and physiological relevance. *Neuroscience* 138: 821–829, 2006.

Browne SH, Kang J, Akk G, Chiang LW, Schulman H, Huguenard JR, Prince DA. Kinetic and pharmacological properties of $GABA_A$ receptors in single thalamic neurons and $GABA_A$ subunit expression. *J Neurophysiol* 86: 2312–2322, 2001.

Calero CI, Vickers E, Cid GM, Aguayo LG, Von Gersdorff H, Calvo DJ. Allosteric modulation of retinal GABA receptors by ascorbic acid. *J Neurosci* 31: 9672–9682, 2011.

Christian CA, Herbert AG, Holt RL, Peng K, Sherwood KD, Pangratz-Fuehrer S, Rudolph U, Huguenard JR. Endogenous positive allosteric modulation of $GABA_A$ receptors by *Diazepam binding inhibitor*. *Neuron* 78: 1063–1074, 2013.

Collins T, Young GT, Millar NS. Competitive binding at a nicotinic receptor transmembrane site of two alpha7-selective positive allosteric modulators with differing effects on agonist-evoked desensitization. *Neuropharmacology* 61: 1306–1313, 2011.

Costa BM, Irvine MW, Fang G, Eaves RJ, Mayo-Martin MB, Skifter DA, Jane DE, Monaghan DT. A novel family of negative and positive allosteric modulators of NMDA receptors. *J Pharmacol Exp Ther* 335: 614–621, 2010.

Cox CL, Huguenard JR, Prince DA. Heterogeneous axonal arborizations of rat thalamic reticular neurons in the ventrobasal nucleus. *J Comp Neurol* 366: 416–430, 1996.

Crabtree JW, Collingridge GL, Isaac JT. A new intrathalamic pathway linking modality-related nuclei in the dorsal thalamus. *Nat Neurosci* 1: 389–394, 1998.

Davie JT, Kole MH, Letzkus JJ, Rancz EA, Spruston N, Stuart GJ, Häusser M. Dendritic patch-clamp recording. *Nat Protoc* 1: 1235–1247, 2006.

Davies PA. Allosteric modulation of the $5\text{-}HT_3$ receptor. *Curr Opin Pharmacol* 11: 75–80, 2011.

Deschenes M, Madariaga-Domich A, Steriade M. Dendrodendritic synapses in the cat reticularis thalami nucleus: a structural basis for thalamic spindle synchronization. *Brain Res* 334: 165–168, 1985.

Faghih R, Gopalakrishnan M, Briggs CA. Allosteric modulators of the alpha7 nicotinic acetylcholine receptor. *J Med Chem* 51: 701–712, 2008.

Fritschy JM, Mohler H. $GABA_A$-receptor heterogeneity in the adult rat brain: differential regional and cellular distribution of seven major subunits. *J Comp Neurol* 359: 154–194, 1995.

Fucile S, Miledi R, Eusebi F. Effects of cyclothiazide on GluR1/AMPA receptors. *Proc Natl Acad Sci USA* 103: 2943–2947, 2006.

Galarreta M, Hestrin S. Properties of $GABA_A$ receptors underlying inhibitory synaptic currents in neocortical pyramidal neurons. *J Neurosci* 17: 7220–7227, 1997.

Hadingham KL, Garrett EM, Wafford KA, Bain C, Heavens RP, Sirinathsinghji DJ, Whiting PJ. Cloning of cDNAs encoding the human gamma-aminobutyric acid type A receptor alpha6 subunit and characterization of the pharmacology of alpha6-containing receptors. *Mol Pharmacol* 49: 253–259, 1996.

Hall CN, Klein-Flügge MC, Howarth C, Attwell D. Oxidative phosphorylation, not glycolysis, powers presynaptic and postsynaptic mechanisms underlying brain information processing. *J Neurosci* 32: 8940–8951, 2012.

Hamill OP, Marty A, Neher E, Sakmann B, Sigworth FJ. Improved patch-clamp techniques for high-resolution current recording from cells and cell-free membrane patches. *Pflügers Arch* 391: 85–100, 1981.

Houser CR, Vaughn JE, Barber RP, Roberts E. GABA neurons are the major cell type of the nucleus reticularis thalami. *Brain Res* 200: 341–354, 1980.

Huguenard JR, Prince DA. Clonazepam suppresses $GABA_B$-mediated inhibition in thalamic relay neurons through effects in nucleus reticularis. *J Neurophysiol* 71: 2576–2581, 1994.

Huntsman MM, Leggio MG, Jones EG. Nucleus-specific expression of $GABA_A$ receptor subunit mRNAs in monkey thalamus. *J Neurosci* 16: 3571–3589, 1996.

Huntsman MM, Porcello DM, Homanics GE, DeLorey TM, Huguenard JR. Reciprocal inhibitory connections and network synchrony in the mammalian thalamus. *Science* 283: 541–543, 1999.

Isaacson JS, Solís JM, Nicoll RA. Local and diffuse synaptic actions of GABA in the hippocampus. *Neuron* 10: 165–75, 1993.

Jia F, Pignataro L, Schofield CM, Yue M, Harrison NL, Goldstein PA. An extrasynaptic $GABA_A$ receptor mediates tonic inhibition in thalamic VB neurons. *J Neurophysiol* 94: 4491–4501, 2005.

Johnstone TB, Gu Z, Yoshimura RF, Villegier AS, Hogenkamp DJ, Whittemore ER, Huang JC, Tran MB, Belluzzi JD, Yakel JL, Gee KW. Allosteric modulation of related ligand-gated ion channels synergistically induces long-term potentiation in the hippocampus and enhances cognition. *J Pharmacol Exp Ther* 336: 908–915, 2011.

Jones EG. Some aspects of the organization of the thalamic reticular complex. *J Comp Neurol* 162: 285–308, 1975.

Jones MV, Westbrook GL. Shaping of IPSCs by endogenous calcineurin activity. *J Neurosci* 17: 7626–7633, 1997.

Kaneda M, Farrant M, Cull-Candy SG. Whole-cell and single-channel currents activated by GABA and glycine in granule cells of the rat cerebellum. *J Physiol* 485.2: 419–435, 1995.

Karakas E, Simorowski N, Furukawa H. Subunit arrangement and phenylethanolamine binding in GluN1/GluN2B NMDA receptors. *Nature* 475: 249–253, 2011.

Léna C, Changeux JP. Allosteric modulations of the nicotinic acetylcholine receptor. *Trends Neurosci* 16: 181–186, 1993.

Lipinski HG, Bingmann D. Diffusion in slice preparations bathed in unstirred solutions. *Brain Res* 437: 26–34, 1987.

Macdonald RL, Olsen RW. $GABA_A$ receptor channels. *Annu Rev Neurosci* 17: 569–602, 1994.

Mody I, Pearce RA. Diversity of inhibitory neurotransmission through $GABA_A$ receptors. *Trends Neurosci* 27: 569–575, 2004.

Möhler H, Crestani F, Rudolph U. $GABA_A$-receptor subtypes: a new pharmacology. *Curr Opin Pharmacol* 1: 22–25, 2001.

Mony L, Kew JN, Gunthorpe MJ, Paoletti P. Allosteric modulators of NR2B-containing NMDA receptors: molecular mechanisms and therapeutic potential. *Br J Pharmacol* 157: 1301–1317, 2009.

O'Connor JJ, Wu J, Rowan MJ, Anwyl R. Potentiation of *N*-methyl-D-aspartate-receptor-mediated currents detected using the excised patch technique in the hippocampal dentate gyrus. *Neuroscience* 69: 363–369, 1995.

Pan ZH, Bähring R, Grantyn R, Lipton SA. Differential modulation by sulfhydryl redox agents and glutathione of GABA- and glycine-evoked currents in rat retinal ganglion cells. *J Neurosci* 15: 1384–1391, 1995.

Perrais D, Ropert N. Effect of zolpidem on miniature IPSCs and occupancy of postsynaptic $GABA_A$ receptors in central synapses. *J Neurosci* 19: 578–588, 1999.

Petrini EM, Zacchi P, Barberis A, Mozrzymas JW, Cherubini E. Declusterization of $GABA_A$ receptors affects the kinetic properties of GABAergic currents in cultured hippocampal neurons. *J Biol Chem* 278: 16271–16279, 2003.

Pinault D, Smith Y, Deschenes M. Dendrodendritic and axoaxonic synapses in the thalamic reticular nucleus of the adult rat. *J Neurosci* 17: 3215–3233, 1997.

Porcello DM, Huntsman MM, Mihalek RM, Homanics GE, Huguenard JR. Intact synaptic GABAergic inhibition and altered neurosteroid modulation of thalamic relay neurons in mice lacking delta subunit. *J Neurophysiol* 89: 1378–1386, 2003.

Pritchett DB, Luddens H, Seeburg PH. Type I and type II $GABA_A$-benzodiazepine receptors produced in transfected cells. *Science* 245: 1389–1392, 1989a.

Pritchett DB, Sontheimer H, Shivers BD, Ymer S, Kettenmann H, Schofield PR, Seeburg PH. Importance of a novel $GABA_A$ receptor subunit for benzodiazepine pharmacology. *Nature* 338: 582–585, 1989b.

Rudolph U, Möhler H. Analysis of $GABA_A$ receptor function and dissection of the pharmacology of benzodiazepines and general anesthetics through mouse genetics. *Annu Rev Pharmacol Toxicol* 44: 475–498, 2004.

Sakmann B, Neher E. *Single-Channel Recording*. New York: Springer, 2009.

Scanziani M. GABA spillover activates postsynaptic $GABA_B$ receptors to control rhythmic hippocampal activity. *Neuron* 25: 673–681, 2000.

Schofield CM, Huguenard JR. GABA affinity shapes IPSCs in thalamic nuclei. *J Neurosci* 27: 7954–7962, 2007.

Schofield CM, Kleiman-Weiner M, Rudolph U, Huguenard JR. A gain in $GABA_A$ receptor synaptic strength in thalamus reduces oscillatory activity and absence seizures. *Proc Natl Acad Sci USA* 106: 7630–7635, 2009.

Schwartz TW, Holst B. Allosteric enhancers, allosteric agonists and ago-allosteric modulators: where do they bind and how do they act? *Trends Pharmacol Sci* 28: 366–373, 2007.

Sheffler DJ, Gregory KJ, Rook JM, Conn PJ. Allosteric modulation of metabotropic glutamate receptors. *Adv Pharmacol* 62: 37–77, 2011.

Shu Y, McCormick DA. Inhibitory interactions between ferret thalamic reticular neurons. *J Neurophysiol* 87: 2571–2576, 2002.

Steriade M. Sleep, epilepsy and thalamic reticular inhibitory neurons. *Trends Neurosci* 28: 317–324, 2005.

Sur C, Farrar SJ, Kerby J, Whiting PJ, Atack JR, McKernan RM. Preferential coassembly of alpha4 and delta subunits of the gamma-aminobutyric acid A receptor in rat thalamus. *Mol Pharmacol* 56: 110–115, 1999.

Syková E, Nicholson C. Diffusion in brain extracellular space. *Physiol Rev* 88: 1277–1340, 2008.

Thompson SM, Gähwiler BH. Effects of the GABA uptake inhibitor tiagabine on inhibitory synaptic potentials in rat hippocampal slice cultures. *J Neurophysiol* 67: 1698–1701, 1992.

Wafford KA, Thompson SA, Thomas D, Sikela J, Wilcox AS, Whiting PJ. Functional characterization of human gamma-aminobutyric acid A receptors containing the alpha4 subunit. *Mol Pharmacol* 50: 670–678, 1996.

Wang H, Bedford FK, Brandon NJ, Moss SJ, Olsen RW. $GABA_A$-receptor-associated protein links $GABA_A$ receptors and the cytoskeleton. *Nature* 397: 69–72, 1999.

Wisden W, Laurie DJ, Monyer H, Seeburg PH. The distribution of 13 $GABA_A$ receptor subunit mRNAs in the rat brain. I. Telencephalon, diencephalon, mesencephalon. *J Neurosci* 12: 1040–1062, 1992.

Yang CR, Svensson KA. Allosteric modulation of NMDA receptor via elevation of brain glycine and D-serine: the therapeutic potentials for schizophrenia. *Pharmacol Ther* 120: 317–332, 2008.

Yévenes GE, Zeilhofer HU. Molecular sites for the positive allosteric modulation of glycine receptors by endocannabinoids. *PLoS One* 6: e23886, 2011.

Zhang SJ, Huguenard JR, Prince DA. $GABA_A$ receptor-mediated Cl^- currents in rat thalamic reticular and relay neurons. *J Neurophysiol* 78: 2280–2286, 1997.